ACS OMEGA

http://pubs.acs.org/journal/acsodf

Article

Electrochemical Carbamazepine Aptasensor for Therapeutic Drug Monitoring at the Point of Care

Saeromi Chung, Naveen K. Singh, Valentin K. Gribkoff, and Drew A. Hall*

Cite This: *ACS Omega* 2022, 7, 39097−39106

Read Online

ACCESS | Metrics & More | Article Recommendations | Supporting Information

ABSTRACT: Monitoring the anti-epileptic drug carbamazepine (CBZ) is crucial for proper dosing, optimizing a patient's clinical outcome, and managing their medication regimen. Due to its narrow therapeutic window and concentration-related toxicity, CBZ is prescribed and monitored in a highly personalized manner. We report an electrochemical conformation-changing aptasensor with two assay formats: a 30 min assay for routine monitoring and a 5 min assay for rapid emergency testing. To enable "sample-to-answer" testing, a de novo CBZ aptamer (K_d < 12 nM) with conformational switching due to a G-quadruplex motif was labeled with methylene blue and immobilized on a gold electrode. The electrode fabrication and detection conditions were optimized using electrochemical techniques and visualized by atomic force microscopy (AFM). The aptasensor performance, including reproducibility, stability, and interference, was characterized using electrochemical impedance spectroscopy and voltammetry techniques. The aptasensor exhibited a wide dynamic range in buffer (10 nM to 100 μM) with limits of detection of 1.25 and 1.82 nM for the 5 and 30 min assays, respectively. The clinical applicability is demonstrated by detecting CBZ in finger prick blood samples (<50 μL). The proposed assays provide a promising method to enable point-of-care monitoring for timely personalized CBZ dosing.

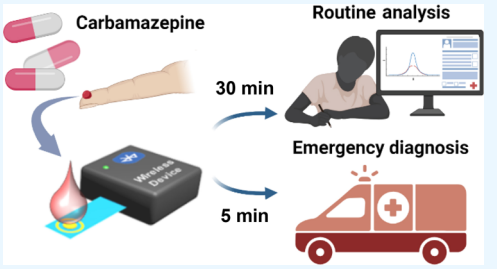

INTRODUCTION

Carbamazepine (CBZ), marketed in the U.S. under the brand names Tegretol, Tegretol XR, Epitol, and Carbatrol, is an FDA-approved antiseizure and analgesic drug widely used to treat partial seizures with complex symptomatology, tonic-clonic seizures, trigeminal neuralgia, and bipolar disorder.[1,2] It is also prescribed to patients with neuromyotonia, schizophrenia, post-traumatic stress disorder, and attention-deficit hyperactivity disorder.[3] CBZ, a tricyclic compound comprising two benzene rings connected by an azepine with a short side chain (236.27 g/mol), acts on the brain and nervous system to control abnormal nerve impulses causing seizures and neurological-derived disorders by blocking ion channels.[4−6] Despite all its benefits, it can cause troubling, disabling, and potentially life-threatening complications, which can be difficult to mitigate clinically because the target therapeutic range is extremely narrow (4−12 mg/L; 16.9−50.8 μM) and severe concentration-related toxicity (i.e., combativeness, hallucinations, chorea, coma, and even death)[7−9] can occur even within the therapeutic range. Furthermore, pharmacokinetics influence proper dosing when treating multiple diseases and in multidrug regimens, as is common in treating epilepsy.[10] Thus, CBZ is a powerful drug but requires careful dosing, often personalized due to multidrug regimens, within a narrow therapeutic window, and routine monitoring is critical to ensure safety and efficacy.

Several analytical techniques have been reported to detect CBZ, such as high-performance liquid chromatography,[11,12] mass spectrometry (MS),[2,13] liquid chromatography coupled with mass spectrometry (LC−MS),[8,14] gas chromatography (GC),[15] capillary chromatography,[16] chemiluminescence,[17] and spectrophotometry.[18] These methods require time-consuming pretreatment processes and sophisticated instrumentation with high per-assay costs, relegating them to centralized laboratory-based tests.[19,20] Such methods cannot be applied for rapid, point-of-care therapeutic drug monitoring. Several attempts at portable assay formats using electrochemical techniques to rapidly detect CBZ and its metabolites have been proposed to overcome the aforementioned limitations.[20,21] Direct electrochemical methods rely on target reduction/oxidation (redox) without an affinity reagent for quantification.[3,22−25] Such direct electrochemical methods are simple, easy, and fast; however, the high oxidation (>0.7 V) and low reduction (<−2.0 V) potentials of CBZ[24,25] lead to significant false positives from other electroactive small molecules (i.e., ascorbic acid, uric acid, dopamine, oxygen, etc.) present at high concentrations in serum. Therefore, these electroactive molecules can overshadow the CBZ signal in the therapeutic range, resulting in challenges with measurements in complex biofluids. Electrochemical molecular imprinting

Received: August 1, 2022
Accepted: September 22, 2022
Published: October 17, 2022

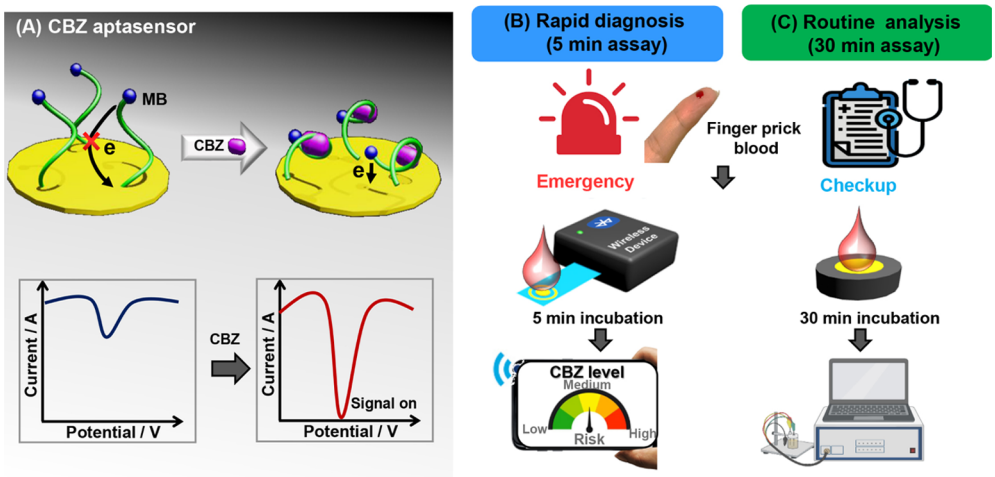

Figure 1. Electrochemical CBZ aptasensor overview. (A) Sensing scheme of the CBZ aptasensor. Workflow for (B) 5 min rapid assay and (C) 30 min assay for routine analysis.

polymer (MIP) sensors, a state-of-the-art process for producing artificial biomimetic receptors, were reported with embedded signal indicators to improve the low specificity of direct detection.[26,27] Although MIP sensors are low-cost and fast, they are less selective than antibodies and have a heterogeneous distribution of binding sites.[28] Thus, despite the numerous techniques developed for CBZ detection, there is still a need for a rapid point-of-care assay that can be run outside of a centralized lab so that treating physicians can institute rapid dosage adjustments.[29−32]

This work uses an aptamer as an affinity reagent to overcome the prior work's lack of specificity and high oxidation potential. Aptamers are artificial oligonucleotides selected in vitro and possess a high binding affinity to their target, ranging from small molecules to cells.[33−35] Aptamers can be used in various applications (e.g., medical biology, microbiology, medicine, analytical chemistry, etc.) due to their high specificity and selectivity.[36−39] Compared to antibodies, the gold standard in affinity assays, aptamers have several unique properties (i.e., temperature stability, in vitro synthesis, ease of chemical modification, longer shelf life, etc.).[40] In particular, aptamer-based biosensors (aptasensors) are being investigated for small molecules (<10 kDa), such as CBZ, which do not have enough immunogenicity to generate a specific antibody.[41,42] Electrochemical aptasensors utilize a target binding-induced conformation change in the aptamer structure, leading to a change in electron transfer between a distal-appended redox tag and an electrode surface.[43,44] Thus, the target−aptamer interaction is transduced into a voltammetric signal that quantifies the amount of the target present in the sample. This electrochemical signaling aptamer enables sample-to-answer testing, even in undiluted blood, because of its folding nature.[43,45] Hence, developing an aptamer-based electrochemical sensor is important in realizing point-of-care testing that is ideally portable, sensitive, affordable, and reliable.[46−48]

This paper presents a conformation-switching electrochemical aptasensor for detecting CBZ for the first time. Our strategy uses a de novo DNA aptamer selected against CBZ with a high affinity (K_d < 12 nM) and specificity that was modified with a thiol group on the 5′-end for immobilization on the gold sensing electrode and a methylene blue (MB) tag on the 3′-end for readout (Figure 1A). This conformation-changing aptamer provides a "sample-to-answer" readout without secondary labeling, as needed in many other affinity assays.[49] In the presence of CBZ, target binding forms a G-quadruplex structure that brings the MB close to the electrode. This proximity increases the electron transfer rate and, thus, the redox current. Two assay formats were developed: a 30 min assay for routine monitoring and a 5 min assay for rapid emergency testing, as shown in Figure 1B,C. The developed assays were verified in contrived biofluid samples. Such assays would allow professionals to rapidly make critical decisions while increasing efficiency and improving the overall patient care.

MATERIALS AND METHODS

Reagents and Instruments. Tris[2-carboxyethyl] phosphine (TCEP; #C4706), magnesium chloride ($MgCl_2$; #208337), calcium chloride ($CaCl_2$; #C5670), phosphate-buffered saline (PBS; #P5493), nuclease-free water (#3098), human serum albumin (HSA; #12667), human serum (#H9614), CBZ (#94496), 6-mercapto-1-hexanol (#725226), 2-mercaptoethanol (2ME) (#M6250), sulfuric acid (#339741), uric acid (UA; #U2625), ascorbic acid (AA; #A5960), diclofenac (#SML3086), and triamcinolone (#1676000) were purchased from Sigma-Aldrich. Reference materials for CBZ 10,11-epoxide (#C-121), oxcarbazepine (#O-025), doxepin (#D-060), amitriptyline (#A-923), protriptyline (#P-903), 10,11-dihydro-10-hydroxycarbamazepine (#D-091), and atenolol (#PHR1909) were acquired from Supelco. Glucose (#A16828) and hydrogen peroxide (H_2O_2; #HX0635-3) were purchased from Thermo Fisher Scientific. The proprietary CBZ-specific single-stranded DNA aptamer modified with a disulfide bond at the 5′ end and MB at the 3′ end (5′-*S*-*S*-TTTTTT-CGA GGC TCT CGG GAC GAC GGG GCA CGG GCC TCT GGG TCG GCA TGG CCC GTC GTC CCG CCT TTA GGA TTT ACA G-MB-3′) was synthesized by Integrated DNA Technologies (IDT). Dulbecco's PBS (dPBS) solution was prepared by adding 0.9 mM $MgCl_2$ and 0.5 mM $CaCl_2$ in 1× PBS and filtering using a 0.22 μm syringe filter. We prepared a stock solution of 250 mM CBZ in a 20:80 ratio of methanol/dPBS. The sample was then prepared after serially diluting the working stock to final concentrations.

Electrochemical impedance spectroscopy (EIS), cyclic voltammetry (CV), differential pulse voltammetry, and square

https://doi.org/10.1021/acsomega.2c04865
ACS Omega 2022, 7, 39097−39106

wave voltammetry (SWV) measurements were performed using a PalmSens4 potentiostat (PalmSens BV, The Netherlands). Electrochemical experiments were conducted using a gold (Au) working electrode (BASi, #MF-2114), a silver/silver chloride (Ag/AgCl) reference electrode, and a platinum (Pt) wire as the counter electrode (CH Instruments, #CHI115). For the 5 min assay, screen-printed electrodes (SPEs) (Metrohm, #C223AT) were used with a 1.6 mm diameter Au working electrode. Atomic force microscopy (AFM) imaging was performed in the tapping mode using a Veeco scanning probe microscope with a Nanoscope IV controller (Veeco Instruments, Woodbury, NY, USA). AFM images were taken in air at room temperature with controlled humidity. Images and roughness values were analyzed using Veeco Instruments software.

Aptamer Selection. Single-stranded DNA (ssDNA) aptamers were selected from a large ssDNA library, synthesized by IDT, by Aptagen, LLC (Jacobus, PA), for candidate selection. Criteria for selection included high affinity and specificity for binding to CBZ in PBS and serum and low binding affinity for the structurally related compounds oxcarbazepine and the metabolite carbamazepine-10,11-epoxide. Selection employed a systematic evolution of ligands by exponential enrichment (SELEX) process,[50,51] in which a hairpin ssDNA library is captured onto magnetic beads through a constant domain and released from the beads as a result of structural changes in response to target binding. Aptagen performed the identification of CBZ-binding aptamers and their initial characterization. Six rounds of selection were performed, followed by three rounds of parallel assessment. Initial selection rounds were performed with the target in PBS, and the final three selection rounds were performed with CBZ in serum. The parallel rounds divided the enriched library into three aliquots for counter screening and affinity testing at low target concentrations.

Approximately 700 sequences were identified by SELEX and examined for their potential to form G-quadruplex structures using a bioinformatics protocol.[53] Those with a high probability of forming a G-quadruplex structure, 53 of the 700, were considered high priority. These 53 structures were probed using the QGRS Mapper software[52] to confirm the likelihood of the G-quadruplex formation via a G-Score produced by the algorithm. Five candidates were selected based on their structural features and high G-scores. The candidate with the highest G-score was subsequently used in all the experiments in these studies.

CBZ Aptasensor Preparation. The Au electrodes were first polished with alumina powder (0.1 and 0.05 μm). After sonicating the electrodes with water and ethanol for 1 min, the electrodes were treated in piranha solution (a mixture of a 3:1 ratio of H_2SO_4/H_2O_2) for 10 min. Safety note: Extreme caution is required when handling and using the corrosive piranha solution. The electrodes were then rinsed thoroughly with water for 3 min and electrochemically cleaned in 0.5 M H_2SO_4 by potential cycling from 0 to 1.4 V for 20 cycles at 0.1 V/s. A 1 μM concentration of the aptamer was prepared by incubating 10 μM aptamer and 100 μM TCEP in dPBS for 2 h at room temperature to reduce the disulfide bonds. The thiol-activated aptamers were then drop-cast on the Au working electrode surface and incubated in a humidity chamber overnight. 10 mM 2ME was placed on the aptasensor for 30 min to remove the unbound aptamer and block the sensor surface.[44] Lastly, the electrodes were gently washed with 1× PBS and kept in a 4 °C humidity chamber until use. The stepwise sensor modification was monitored using CV and EIS with 5 mM $[Fe(CN)_6]^{4-/3-}$ in 0.1 M PBS and SWV in 0.1 M PBS. All electrodes were examined in a blank solution at every immobilization step to select those with a similar response.

Aptasensor Assays. Calibration plots were generated by spiking various concentrations of CBZ in buffer, serum, and 20× diluted blood samples. For each measurement, 50 μL of the sample was incubated on the working electrode for 5 or 30 min and then gently washed with PBS. Voltammograms were measured using SWV in dPBS solution from 0.15 to −0.55 V with a 5 Hz frequency and a 50 mV amplitude. For 5 min sample tests, there was no washing. Specificity was evaluated by measuring CBZ analogues, metabolites, and other compounds having a similar chemical structure to CBZ (i.e., carbamazepine 10,11-epoxide, oxcarbazepine, doxepin, amitriptyline, protriptyline, 10,11-dihydro-10-hydroxycarbamazepine). Following the same process described above, these analogues were assayed at 1 and 10 μM. Other medications (i.e., triamcinolone, atenolol, and diclofenac) and electroactive biomolecules (i.e., glucose, uric acid, and ascorbic acid) were also investigated at physiological concentrations.

Statistical Analysis. All measurements were performed in at least triplicate with independent sensors fabricated and examined under similar conditions. All data shown are mean values, with the error bars representing one standard deviation (SD). Statistical analysis was performed using Origin 9.0. The limit of detection (LOD) was calculated using the slope method, where LOD = 3 × SD of the blank/slope.[35]

RESULTS AND DISCUSSION

This assay aims to create an easy-to-use sensor for CBZ monitoring that allows for a wide variety of clinical applications with the fewest steps for sensor fabrication and operations at a low cost. The 30 min assay is intended for routine monitoring to screen the drug's levels in the patients because this drug must be maintained within a narrow therapeutic range (16.9−50.8 μM). Below this range, CBZ is no longer effective, and the recurrence of symptoms (i.e., seizures, mania, or pain) is possible. Additionally, high levels of CBZ cause toxic side effects. Therefore, CBZ dosages must be adjusted carefully to reach a steady concentration that varies from person to person and can change over time. Compared to the currently available CBZ testing, which relies on the blood sample drawn from a vein, this assay uses a small volume of finger prick blood samples. Due to the life-threatening concentration-related CBZ toxicity and emergent seizure, a rapid assay format was designed for emergency care decisions (i.e., gastrointestinal decontamination, extracorporeal elimination, etc.).

CBZ Aptamer. The DNA aptamer was selected through a SELEX process. Supporting Information Figure S1A shows the secondary structures and Gibbs free energies (ΔG = −22.37 kcal/mol) predicted by M-fold at 25 °C in 150 mM Na^+ and 0.5 mM Mg^{2+}. The CBZ aptamer has a G-quadruplex forming region (CGA GGC TCT CGG GAC GAC GGG GCA CGG GCC TCT GGG TCG GCA TGG CCC GTC GTC CCG CCT TTA GGA TTT ACA G), where guanine bases in the G-quadruplex structure are underlined and bolded. We simulated the aptamer binding modes to the target molecule using in silico modeling, as shown in Supporting Information Figure S1B. These results showed that the aptamer formed a hairpin upon binding CBZ, enabling it to be used in a conformation-switching assay format.

https://doi.org/10.1021/acsomega.2c04865
ACS Omega 2022, 7, 39097−39106

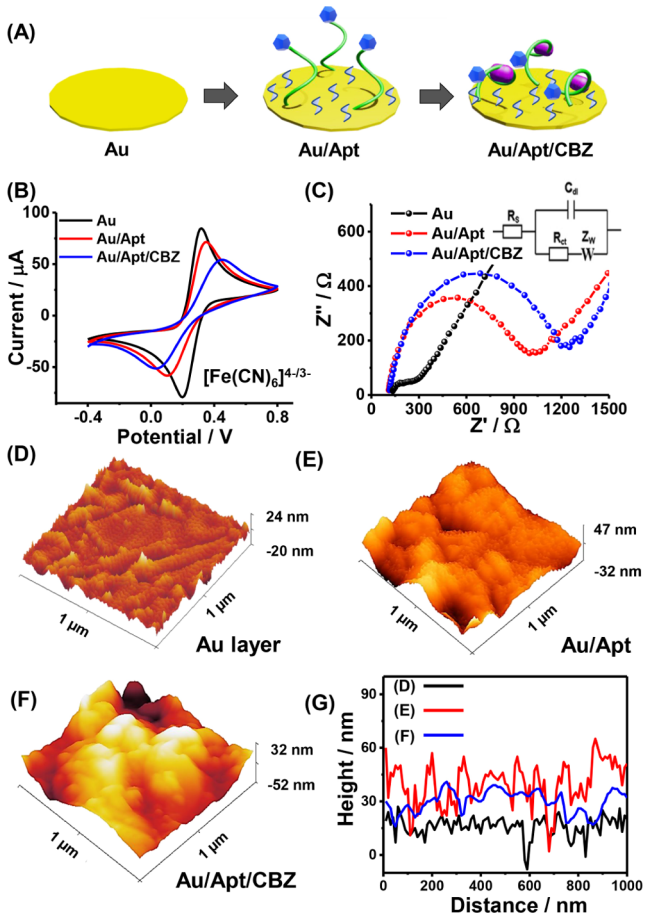

Figure 2. Aptasensor characterization. (A) Illustrations of the sensor fabrication process. (B) Voltammograms during aptasensor fabrication in 5 mM $[Fe(CN)_6]^{4-/3-}$. (C) Nyquist plots during aptasensor fabrication with spiked CBZ in 5 mM $[Fe(CN)_6]^{4-/3-}$. (D–F) AFM topographic images of the electrode surface. (G) Corresponding surface roughness height profiles extracted from AFM images.

Aptasensor Characterization. The CBZ aptasensor fabrication scheme is illustrated in Figure 2A, where the sensor surface is decorated with aptamers and 2ME after cleaning the gold electrode. Stepwise characterization of the assembly was investigated using CV and EIS to validate the aptamer response toward CBZ. Voltammograms were recorded in 5 mM $[Fe(CN)_6]^{4-/3-}$ after each step, as shown in Figure 2B. The electrodes exhibited well-defined reversible ferri-/ferro-cyanide redox peaks. The ferri-/ferro-cyanide peak current decreased after immobilizing the aptamer, indicating that the aptamer was successfully anchored to the surface via a Au–S bond. Lastly, the current was further reduced when exposed to the analyte, verifying that the aptamer recognized CBZ.

The aptasensor was then studied using EIS—an electrochemical technique often used to investigate the electrode surface properties, specifically the change in charge transfer resistance (R_{ct}) due to the probe–target interaction.[54] Figure 2C shows a Nyquist plot, where the impedance's imaginary (Z'') and real (Z') parts are plotted and fitted with a Randles circuit. The bare gold electrodes exhibited a low R_{ct} value (152 Ω) due to gold's high electron transfer capability. After aptamer modification, R_{ct} increased by ∼6× (947 Ω) and increased further in the presence of CBZ (1076 Ω). These data are in close agreement with the CV measurements.

We also imaged the electrode surface using an atomic force microscope to quantify the morphology changes during fabrication. Figure 2D shows an image of a freshly cleaned gold surface with a reasonably smooth surface (<24 nm_{pk}, 4.16 ± 0.53 nm_{rms} roughness). The gold surface exhibited small defects, likely due to mechanical abrasion or aggressive acid cleaning. After immobilizing the aptamer (Figure 2E), a significant change in the morphology was observed (∼47 nm_{pk}, 8.97 ± 1.05 nm_{rms} roughness) due to the formation of an aptamer monolayer. Finally, the CBZ–aptamer complex exhibited a smoother morphology (<32 nm_{pk}, 66.10 ± 0.65 nm_{rms} roughness), as shown in Figure 2F, indicating conformation switching due to target binding. Such results demonstrate successful sensor fabrication. The surface roughness, as compiled from the AFM height profiles, is shown in Figure 2G. Supporting Information Figure S2 summarizes these measurements, showing their statistical significance.

Optimization. After demonstrating that the aptamer has a high affinity to the target, we optimized the fabrication and sensing conditions using EIS. The changes in R_{ct} were measured after varying the aptamer loading density, CBZ incubation time, pH, and label position (3′ vs 5′). Since the probes' composition should not interfere with the aptamer folding for correct functionality, spacer molecules were added to reduce the aptamers' close packing and offer an adequate space for binding.[44,55] As shown in Supporting Information Figure S3, the aptamer loading density was tested using different aptamer and spacer ratios. Interestingly, aptamer to spacer ratios of 1:1 and 1:2 showed reduced sensitivity to CBZ compared to that of a 1:0 ratio (no spacer). This indicates that the high packing density with this aptamer does not affect the mobility of the MB tag and electron transfer from the unfolded state. This might be due to the steric and electrostatic repulsion between negatively charged nucleotides providing enough space for random coil structure folds into quadruplex structures.[56,57] Thus, the 1:0 ratio was used for all further experiments.

Next, the effect of CBZ incubation time with the aptasensor was studied. Without a label on the aptamer, forming the target–aptamer complex on the electrode inhibits the electron transfer, leading to an increase in R_{ct}.[58] As the incubation time was increased from 0 to 40 min, a gradual increase in R_{ct} was observed, followed by a subsequent plateaue, as shown in Supporting Information Figure S4. A 30 min incubation time was chosen to balance the assay time since it showed 80% of the maximum response. These data also demonstrated that a shorter incubation time was possible for a rapid format assay, where even at 5 min, ∼30% of the maximum signal was observed.

The pH effect on the sensor performance was also studied. As shown in Supporting Information Figure S5, under acidic conditions (pH 5.0), the change in R_{ct} (ΔR_{ct}) before and after the addition of 100 μM CBZ was negligible; however, it increased monotonically up to a pH of 7.4. In basic solutions (pH 8.0), the response decreased. The maximum signal was observed at a pH of 7.4. To select the best orientation of the aptamer and the MB label, we tested aptamers labeled at the 3′- and 5′-ends with various CBZ concentrations (10, 100, and 1000 nM). As shown in Supporting Information Figure S6, the 3′-MB and 5′-thiol aptamer was more responsive (380 nA/nM) than the 5′-MB and 3′-thiol aptamer (160 nA/nM). Hence, we used the 3′-MB modified aptamer at a pH of 7.4 with a 30 min target incubation for all subsequent experiments.

https://doi.org/10.1021/acsomega.2c04865
ACS Omega 2022, 7, 39097–39106

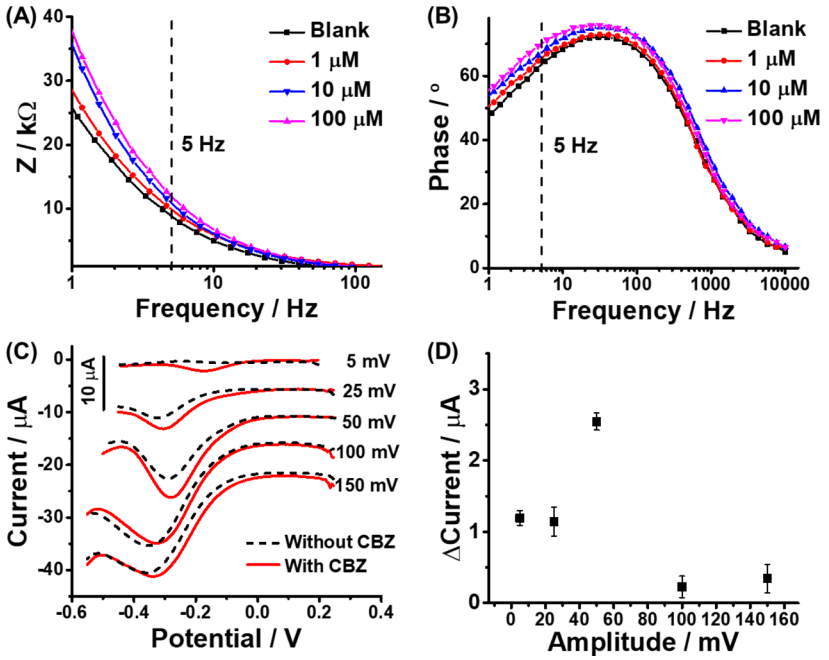

Figure 3. Aptamer conformation switching study. (A) Magnitude and (B) phase of the measured impedance at various CBZ concentrations. (C) Voltammograms recorded at different amplitudes (5−150 mV) with (red solid line) and without CBZ (black dashed line) and (D) differences in peak current vs SWV amplitude.

Because conformation-switching aptasensors rely on a binding-induced signal, which is dependent on the frequency and amplitude of SWV,[59] we optimized the parameters with and without CBZ to maximize the signal gain. Figure 3A,B shows Bode plots for different CBZ concentrations in PBS, where the impedance increases as a function of the target concentration. The largest response appeared at low frequencies (<10 Hz), with no significant difference between 1 and 5 Hz. Therefore, 5 Hz was selected to minimize the measurement time. As the voltammetric response is very sensitive to the square wave amplitude,[59,60] the amplitude was swept from 5 to 150 mV and measured at a fixed CBZ concentration. Figure 3C shows the aptasensor SWV signals with and without CBZ at various amplitudes, and the corresponding peak difference [$\Delta I = I(\mathrm{CBZ}) - I(\mathrm{blank})$, $n = 3$] is shown in Figure 3D. The current was increased from 5 to 50 mV and then reduced. The most significant change was observed at 50 mV and decreased after that, possibly due to incomplete settling of the potential-dependent non-Faradaic current. These optimized values (5 Hz and 50 mV) were used for all further experiments.

CBZ Detection. CBZ (10 nM to 100 μM) was incubated on the sensor for 5 and 30 min to assess the aptasensor performance. Figure 4A,C shows the responses in buffer solution. The response is linear in both cases, with the 30 min assay exhibiting a higher sensitivity (395 vs 69 nA/nM) and less variation. Testing higher concentrations is not possible due to aqueous solubility limits. These data agree with EIS measurements, which used an unlabeled aptamer to exclude other effects from the electroactive label that may cause a false signal on EIS (Supporting Information Figure S7). The measurements were then repeated but this time with CBZ spiked into human serum, as shown in Figure 4B,D. The serum measurements were linear, like the buffer measurements, where the slight difference is likely due to matrix effects (e.g., salt concentrations, pH, etc.). The 5 min assay has 1.25 and 2.12

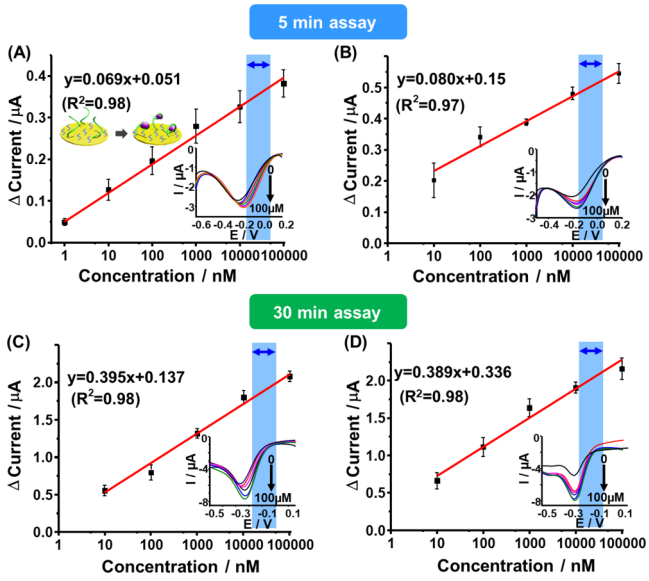

Figure 4. CBZ detection. Calibration plots for the 5 min assay in (A) buffer and (B) spiked serum samples and for the 30 min assay in (C) buffer and (D) spiked serum samples (inset: voltammograms at different CBZ concentrations). The blue shading depicts the therapeutic window.

nM LODs in the buffer and serum, respectively, whereas the 30 min assay has 1.82 and 2.06 nM LODs, respectively. Both assays have a 10 nM to 100 μM linear dynamic range, covering the CBZ therapeutic dose range (16.9−50.8 μM). The CBZ aptasensor's wide dynamic range and high sensitivity enable detection in dilute samples, easing sample collection (low volume) and minimizing matrix effects since the matrix is diluted.

To assess the assay's precision and accuracy, recovery tests were run using CBZ spiked in undiluted serum. The samples

https://doi.org/10.1021/acsomega.2c04865
ACS Omega 2022, 7, 39097−39106

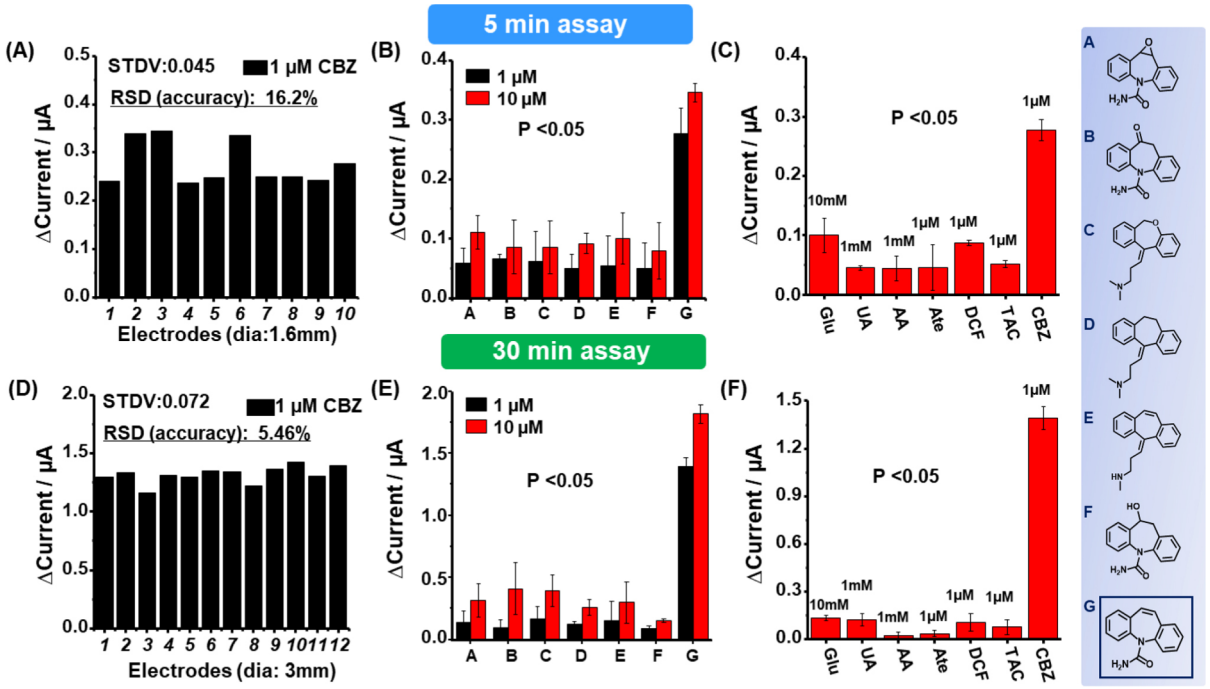

Figure 5. Reproducibility and interference. (A−C) 5 min assay and (D−F) 30 min assay for (A,D) reproducibility, (B,E) interference studies using 1 and 10 μM concentrations of CBZ analogues and CBZ. (A: carbamazepine 10,11-epoxide, B: oxcarbazepine, C: doxepin, D: amitriptyline, E: protriptyline, F: 10,11-dihydro-10-hydroxycarbamazepine, and G: CBZ), and (C,F) electroactive off-target interference.

were prepared at three different CBZ concentrations and run in both assay formats. The percent recovery (Supporting Information Table S1 and Figure S8) was within ±30% and deemed acceptable (76.1−125.9% for the 5 min assay and 82.7−114.5% for the 30 min assay). The accuracy of the 30 min assay is higher than that of the 5 min assay, likely due to the stochasticity stemming from the reduced incubation time.[61] Lastly, three CBZ spiked samples in buffer were prepared and presented blinded. As shown in Supporting Information Table S2 and Figure S9, the mean values of the 5 and 30 min assays, respectively, were as follows: 48.2 and 50.5 μM for sample 1 (true 50 μM), 12.5 and 14.3 μM for sample 2 (true 15 μM), and 20.7 and 21.1 μM for sample 3 (true 20 μM). These data demonstrate that the assay can detect CBZ over the therapeutic range in serum with two different incubation times, one amenable to rapid sample-to-answer readout and a longer incubation time with better accuracy.

Stability, Reproducibility, and Interference Studies. As most nucleic acids are susceptible to nucleases and the surface monolayer desorption, one of the difficulties in measuring clinical samples is the aptasensor's stability in serum and blood.[62−64] To study the aptasensor stability, we incubated the sensors with 100 nM CBZ spiked in undiluted serum at 4 °C (Supporting Information Figure S10A) and 20-fold diluted blood at ambient temperature (Supporting Information Figure S10B). In undiluted serum, the sensor was stable for 90 min, after which the response gradually decreased up to 5 h and lost half of the signal at 12 h. The 12 h aptamer half-life in 4 °C serum is likely due to the low enzyme activities and G-quadruplex structures providing stability against the nucleases.[65,66] Also, such a decay of signal gain might be due to the desorption of the self assembled monolayer (SAM), irreversible reduction of the MB tag, DNA cleavage, and/or non-specific binding of proteins in the sample. The sensors were stable for 30 min in diluted blood at ambient temperature but rapidly decreased with longer incubation times. While sufficient for the proposed assay formats, it may be necessary to improve the aptamer stability by modifying the backbone in future work.[67]

The sensors' reproducibility was evaluated using 10 independent electrodes incubated with 1 μM CBZ in buffer solution for 5 min and then measured. The response of each electrode exhibited a similar current response with a relative standard deviation (RSD) of 16.2%, as shown in Figure 5A. This process was repeated with a 30 min incubation using 10 electrodes and had an RSD of 5.46%, as shown in Figure 5D. The lower variance with the longer incubation time is consistent with the larger error bars observed previously in the calibration plots with the shorter duration assay. It is also worth noting that the sensors used in the 5 min assay format are off-the-shelf SPEs, which have a smaller working electrode area (1.6 mm) than those used for the 30 min assay (3 mm) and are likely contributing to the variation. Both sensors exhibit a high degree of stability and reproducibility.

Next, we studied the potential interference from CBZ analogues, specifically carbamazepine 10,11-epoxide, oxcarbazepine, doxepin, amitriptyline, protriptyline, and 10,11-dihydro-10-hydroxycarbamazepine. The chemical structures of these compounds are shown in Figure 5. These interfering molecules could be present at concentrations equal to or greater than that of CBZ, and therefore, we tested two concentrations of CBZ and each potential interfering structure: 1 and 10 μM. Although the six compounds have similar structures, differing by only one or two functional groups, there were no considerable current changes in the presence of these compounds (P-value < 0.05), as shown in Figure 5B,E, whereas a significant signal was observed for CBZ. Finally, we looked at other electroactive, off-target molecules (i.e., glucose, uric acid, and ascorbic acid) and frequently used medications (i.e., atenolol, diclofenac, and triamcinolone) (Figure 5C,F). Each

https://doi.org/10.1021/acsomega.2c04865
ACS Omega 2022, 7, 39097−39106

concentration was selected at the high end of the physiological range to assess the worst case scenario. Like the CBZ analogues, the off-target molecules induced a considerably smaller response than 1 μM CBZ, even at concentrations up to 10,000× higher. This indicates that the aptamer has a very high selectivity toward CBZ.

Validation. Having demonstrated the reproducibility and selectivity, we next measured CBZ spiked into finger prick blood samples from healthy volunteers. Each sample was diluted 20-fold with dPBS, spiked with CBZ at varying concentrations, and incubated for 5 and 30 min on the electrode. After the incubation, the sample was pipetted and incubated without washing (for the 5 min assay) or washed with dPBS (for the 30 min assay) to prevent coagulation, and voltammograms were recorded using SWV. The response for both assays was linear, with the 5 min assay having a linear range from 100 nM to 100 μM with an LOD of 54.25 nM (Figure 6A) and the 30 min assay having a linear range from

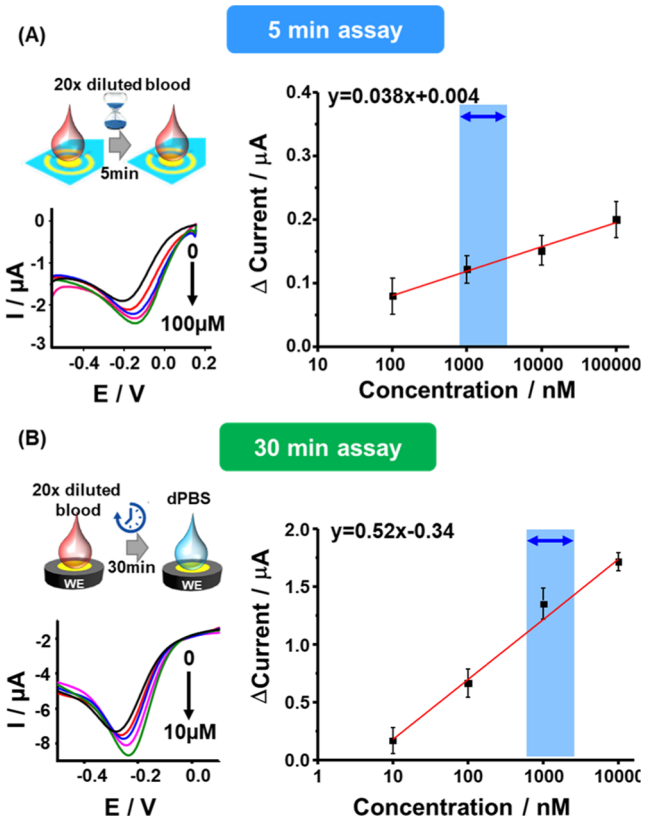

Figure 6. Blood spiking study. (A) 5 min assay in blood spiked samples without the washing step and (B) 30 min assay in 20× diluted blood spiked samples with washing. The blue shading depicts the therapeutic window in 20× diluted blood.

10 nM to 10 μM and an LOD of 2.62 nM (Figure 6B). The ability to directly detect CBZ in diluted blood obviates the need for complex pretreatment steps (e.g., centrifugation, filtering, etc.), enabling the aptasensor to be used at the point of care—a significant advantage compared to the prior state-of-the-art method that only demonstrated such detection in buffer or serum.

Comparison. The reported aptasensor was compared with other CBZ sensors reported in the literature, including electrochemical sensors, fluorescence polarization immunoassay, LC−MS/MS, and dispersive liquid−liquid microextraction, as shown in Supporting Information Table S3. This aptasensor has the broadest dynamic range, covering the therapeutic range of CBZ and the lowest LOD. Most importantly, the proposed assay can detect CBZ in serum or blood without pretreatment steps (i.e., centrifugation, filtering, and mixing with other solvents), which is a significant problem in translating the other approaches to point-of-care assays. The total assay time was comparable to or superior to that of the others. Finally, the developed aptasensor assays could be used with hand-held or benchtop devices, enabling this assay to be brought closer to the patient with a fast turnaround time.

In Supporting Information Table S4, we compare the developed 5 and 30 min assays. Although the dynamic ranges of both assays cover the target therapeutic window for CBZ, the 30 min assay provides a better response and accuracy than the 5 min assay. However, the 5 min assay setup uses disposable electrodes and does not require the washing step, showing the applicability toward a rapid diagnosis in emergency care. Therefore, a 5 min rapid assay is desirable for emergency care decisions to rapidly identify the CBZ concentrations so that medical providers can administer the appropriate medical care in the case of drug poisoning, emergent seizures, and so forth. For therapeutic drug treatment monitoring, CBZ concentrations should be maintained and managed in long-term administered patients because CBZ undergoes autoinduction, in which clearance increases over time following exposure to the drug and interindividual differences in response to CBZ. Therefore, a 30 min assay takes longer than the 5 min assay, but it higher accuracy is appropriate for regular concentration checkups.

CONCLUSIONS

In this study, for the first time to our knowledge, we demonstrated an aptamer-based CBZ sensor where an MB label and a G-quadruplex structure enable a sample-to-answer conformation-switching assay. The electrochemical aptasensor construction was characterized using CV, EIS, and AFM and then optimized to achieve the best response. The developed sensor exhibits a high affinity toward CBZ with minimal off-target binding, allowing it to be used in complex biofluids such as serum and blood with a negligible effect from interfering species. Two versions of the assay, 5 and 30 min incubation times, were characterized and validated. Both assays cover the target therapeutic range for CBZ, with the 30 min assay providing better reproducibility and a lower LOD. Compared to other CBZ assays reported in the literature, this assay exhibits the broadest dynamic range and the lowest LOD. It is also the first assay that removes pretreatment steps, allowing it to be used at the point of need. The CBZ aptasensor was tested in vitro using human serum and human blood, demonstrating the potential for further therapeutic applications. Future efforts will be focused on automating the assays with a small hand-held device for point-of-care testing.

ASSOCIATED CONTENT

Supporting Information

The Supporting Information is available free of charge at https://pubs.acs.org/doi/10.1021/acsomega.2c04865.

CBZ aptamer folding structure, optimization data, spike and recovery data, blinded measurement results, and a comparison with existing CBZ sensors (PDF)

https://doi.org/10.1021/acsomega.2c04865
ACS Omega 2022, 7, 39097−39106

AUTHOR INFORMATION

Corresponding Author

Drew A. Hall − *Department of Electrical and Computer Engineering and Department of Bioengineering, University of California San Diego, La Jolla, California 92093, United States;* orcid.org/0000-0003-0674-074X; Email: drewhall@ucsd.edu

Authors

Saeromi Chung − *Department of Electrical and Computer Engineering, University of California San Diego, La Jolla, California 92093, United States;* orcid.org/0000-0002-6389-9709

Naveen K. Singh − *Department of Electrical and Computer Engineering, University of California San Diego, La Jolla, California 92093, United States;* Present Address: Department of Biomedical Engineering, Pennsylvania State University, State College, PA 16803, United States

Valentin K. Gribkoff − *Mensura Health, Weston, Massachusetts 02493, United States*

Complete contact information is available at: https://pubs.acs.org/10.1021/acsomega.2c04865

Notes

The authors declare the following competing financial interest(s): Mensura Health employs V.K.G., and Mensura Health has filed IP on the reported aptamer.

ACKNOWLEDGMENTS

This work was supported by Mensura Health (formerly known as Therastat). We thank Nancy Hsiung, Steven Schachter, and Charles Keough for their feedback and useful discussions around CBZ treatment.

REFERENCES

(1) García-Espinoza, J. D.; Mijaylova-Nacheva, P.; Avilés-Flores, M. Electrochemical Carbamazepine Degradation: Effect of the Generated Active Chlorine, Transformation Pathways and Toxicity. *Chemosphere* **2018**, *192*, 142−151.

(2) Zhou, S.; Xu, L.; Liu, L.; Kuang, H.; Xu, C. Development of a Monoclonal Antibody-Based Immunochromatographic Assay for the Detection of Carbamazepine and Carbamazepine-10, 11-Epoxide. *J. Chromatogr. B: Anal. Technol. Biomed. Life Sci.* **2020**, *1141*, 122036.

(3) Pruneanu, S.; Pogacean, F.; Biris, A. R.; Ardelean, S.; Canpean, V.; Blanita, G.; Dervishi, E.; Biris, A. S. Novel Graphene-Gold Nanoparticle Modified Electrodes for the High Sensitivity Electrochemical Spectroscopy Detection and Analysis of Carbamazepine. *J. Phys. Chem. C* **2011**, *115*, 23387−23394.

(4) Tolou-Ghamari, Z.; Zare, M.; Habibabadi, J. M.; Najafi, M. R. A Quick Review of Carbamazepine Pharmacokinetics in Epilepsy from 1953 to 2012. *J. Res. Med. Sci.* **2013**, *18*, S81.

(5) Beran, R. G. Carbamazepine -An oldie but a goodie-A clinician's perspective. *Seizure* **2020**, *83*, 243−245.

(6) Pineda-Farias, J. B.; Loeza-Alcocer, J. E.; Nagarajan, V.; Gold, M. S.; Sekula, R. F. A Differential Participation of Voltage Gated Sodium Channels Is Related to the Selective Efficacy of Carbamazepine in Trigeminal Neuralgia. *J. Pain* **2021**, *22*, 583−584.

(7) Fernández-López, L.; Mancini, R.; Rotolo, M.-C.; Navarro-Zaragoza, J.; Hernández Del Rincón, J.-P.; Falcón, M. Carbamazepine Overdose after Psychiatric Conditions: A Case Study for Postmortem Analysis in Human Bone. *Toxics* **2022**, *10*, 322.

(8) Ma, D.; Ji, Z.; Cao, H.; Huang, J.; Zeng, L.; Yin, L. LC-MS3 Strategy for Quantification of Carbamazepine in Human Plasma and Its Application in Therapeutic Drug Monitoring. *Molecules* **2022**, *27*, 1224.

(9) CarbamazepineCasebook in Clinical Pharmacokinetics and Drug DosingAccessPharmacy; McGraw Hill Medical. https://accesspharmacy.mhmedical.com/content.aspx?sectionid=88803447&bookid=1514 (accessed Aug 08, 2021).

(10) Keränen, T.; Sivenius, J. Side Effects of Carbamazepine, Valproate and Clonazepam during Long-Term Treatment of Epilepsy. *Acta Neurol. Scand.* **1983**, *68*, 69−80.

(11) Behbahani, M.; Najafi, F.; Bagheri, S.; Bojdi, M. K.; Salarian, M.; Bagheri, A. Application of surfactant assisted dispersive liquid-liquid microextraction as an efficient sample treatment technique for preconcentration and trace detection of zonisamide and carbamazepine in urine and plasma samples. *J. Chromatogr. A* **2013**, *1308*, 25−31.

(12) Kelmann, R. G.; Kuminek, G.; Teixeira, H. F.; Koester, L. S. Determination of Carbamazepine in Parenteral Nanoemulsions: Development and Validation of an HPLC Method. *Chromatographia* **2007**, *66*, 427−430.

(13) Datar, P. A. Quantitative Bioanalytical and Analytical Method Development of Dibenzazepine Derivative, Carbamazepine: A Review. *J. Pharm. Anal.* **2015**, *5*, 213−222.

(14) Hu, L.; Martin, H. M.; Arce-Bulted, O.; Sugihara, M. N.; Keating, K. A.; Strathmann, T. J. Oxidation of Carbamazepine by Mn(VII) and Fe(VI): Reaction Kinetics and Mechanism. *Environ. Sci. Technol.* **2009**, *43*, 509−515.

(15) Durán-Alvarez, J. C.; Becerril-Bravo, E.; Castro, V. S.; Jiménez, B.; Gibson, R. The Analysis of a Group of Acidic Pharmaceuticals, Carbamazepine, and Potential Endocrine Disrupting Compounds in Wastewater Irrigated Soils by Gas Chromatography−Mass Spectrometry. *Talanta* **2009**, *78*, 1159−1166.

(16) Marziali, E.; Raggi, M. A.; Komarova, N.; Kenndler, E. Octakis-6-sulfato-γ-cyclodextrin as additive for capillary electrokinetic chromatography of dibenzoazepines: Carbamazepine, oxcarbamazepine and their metabolites. *Electrophoresis* **2002**, *23*, 3020−3026.

(17) Lee, S. H.; Li, M.; Suh, J. K. Determination of Carbamazepine by Chemiluminescence Detection Using Chemically Prepared Tris-(2,2'-bipyridine)-ruthenium(III) as Oxidant. *Anal. Sci.* **2003**, *19*, 903−906.

(18) Goudarzy, F.; Zolgharnein, J.; Ghasemi, J. B. Determination and Degradation of Carbamazepine Using G-C3N4@CuS Nanocomposite as Sensitive Fluorescence Sensor and Efficient Photocatalyst. *Inorg. Chem. Commun.* **2022**, *141*, 109512.

(19) Atkins, S.; Jiménez Pérez, R.; Sevilla, J. M.; Blázquez, M.; Pineda, T.; González-Rodríguez, J. Electrochemical Reduction of Carbamazepine in Ethanol and Water Solutions Using a Glassy Carbon Electrode. *Int. J. Electrochem. Sci.* **2013**, *8*, 2056−2068.

(20) Dhanalakshmi, N.; Priya, T.; Thinakaran, N. Highly Electroactive Ce-ZnO/RGO Nanocomposite: Ultra-Sensitive Electrochemical Sensing Platform for Carbamazepine Determination. *J. Electroanal. Chem.* **2018**, *826*, 150−156.

(21) Lin, W. Y.; Pan, M. L.; Wang, H. Y.; Su, Y. O.; Huang, P. W. Analysis of Carbamazepine Serum by Differential Pulse Voltammetry (DPV) and Comparison with Fluorescence Polarization Immunoassay (FPIA): An Animal Study. *Med. Chem. Res.* **2012**, *21*, 4389−4394.

(22) Atkins, S.; Sevilla, J. M.; Blazquez, M.; Pineda, T.; Gonzalez-Rodriguez, J. Electrochemical Behaviour of Carbamazepine in Acetonitrile and Dimethylformamide Using Glassy Carbon Electrodes and Microelectrodes. *Electroanalysis* **2010**, *22*, 2961−2966.

(23) Kalanur, S. S.; Jaldappagari, S.; Balakrishnan, S. Enhanced Electrochemical Response of Carbamazepine at a Nano-Structured Sensing Film of Fullerene-C60 and Its Analytical Applications. *Electrochim. Acta* **2011**, *56*, 5295−5301.

(24) Unnikrishnan, B.; Mani, V.; Chen, S.-M. Highly sensitive amperometric sensor for carbamazepine determination based on electrochemically reduced graphene oxide-single-walled carbon nanotube composite film. *Sens. Actuators, B* **2012**, *173*, 274−280.

https://doi.org/10.1021/acsomega.2c04865
ACS Omega 2022, 7, 39097−39106

(25) Veiga, A.; Dordio, A.; Carvalho, A. J. P.; Teixeira, D. M.; Teixeira, J. G. Ultra-Sensitive Voltammetric Sensor for Trace Analysis of Carbamazepine. *Anal. Chim. Acta* **2010**, *674*, 182−189.
(26) Chen, C.; Wang, Y.; Ding, S.; Hong, C.; Wang, Z. A Novel Sensitive and Selective Electrochemical Sensor Based on Integration of Molecularly Imprinted with Hollow Silver Nanospheres for Determination of Carbamazepine. *Microchem. J.* **2019**, *147*, 191−197.
(27) Song, Z.; Zhai, X.; Jiang, C.; Chen, R.; Ye, S.; Tong, J.; Dramou, P.; He, H. Sensitive and Selective Detection of Carbamazepine in Serum Samples by Bionic Double-Antibody Sandwich Method Based on Cucurbit[7]Uril and Molecular Imprinted Polymers. *Biosens. Bioelectron.* **2022**, *203*, 114037.
(28) Xu, Z. x.; Gao, H. j.; Zhang, L. m.; Chen, X. q.; Qiao, X. g. The Biomimetic Immunoassay Based on Molecularly Imprinted Polymer: A Comprehensive Review of Recent Progress and Future Prospects. *J. Food Sci.* **2011**, *76*, R69−R75.
(29) Yu, Z.; Tang, Y.; Cai, G.; Ren, R.; Tang, D. Paper Electrode-Based Flexible Pressure Sensor for Point-of-Care Immunoassay with Digital Multimeter. *Anal. Chem.* **2019**, *91*, 1222−1226.
(30) Yu, Z.; Cai, G.; Tong, P.; Tang, D. Saw-Toothed Microstructure-Based Flexible Pressure Sensor as the Signal Readout for Point-of-Care Immunoassay. *ACS Sens.* **2019**, *4*, 2272−2276.
(31) Teymourian, H.; Parrilla, M.; Sempionatto, J. R.; Montiel, N. F.; Barfidokht, A.; Van Echelpoel, R.; De Wael, K.; Wang, J. Wearable Electrochemical Sensors for the Monitoring and Screening of Drugs. *ACS Sens.* **2020**, *5*, 2679−2700.
(32) Barfidokht, A.; Mishra, R. K.; Seenivasan, R.; Liu, S.; Hubble, L. J.; Wang, J.; Hall, D. A. Wearable Electrochemical Glove-Based Sensor for Rapid and on-Site Detection of Fentanyl. *Sens. Actuators, B* **2019**, *296*, 126422.
(33) Ellington, A. D.; Szostak, J. W. In vitro selection of RNA molecules that bind specific ligands. *Nature* **1990**, *346*, 818−822.
(34) Fan, K.; Zhu, J.; Wu, X.; Zhang, X.; Wang, S.; Wen, W. A Flexible Label-Free Electrochemical Aptasensor Based on Target-Induced Conjunction of Two Split Aptamers and Enzyme Amplification. *Sens. Actuators, B* **2022**, *363*, 131766.
(35) Singh, N. K.; Chung, S.; Sveiven, M.; Hall, D. A. Cortisol Detection in Undiluted Human Serum Using a Sensitive Electrochemical Structure-Switching Aptamer over an Antifouling Nanocomposite Layer. *ACS Omega* **2021**, *6*, 27888−27897.
(36) Ruscito, A.; DeRosa, M. C. Small-Molecule Binding Aptamers: Selection Strategies, Characterization, and Applications. *Front. Chem.* **2016**, *4*, 14.
(37) Qiu, Z.; Shu, J.; Liu, J.; Tang, D. Dual-Channel Photoelectrochemical Ratiometric Aptasensor with up-Converting Nanocrystals Using Spatial-Resolved Technique on Homemade 3D Printed Device. *Anal. Chem.* **2019**, *91*, 1260−1268.
(38) Cai, G.; Yu, Z.; Ren, R.; Tang, D. Exciton-Plasmon Interaction between AuNPs/Graphene Nanohybrids and CdS Quantum Dots/TiO2 for Photoelectrochemical Aptasensing of Prostate-Specific Antigen. *ACS Sens.* **2018**, *3*, 632−639.
(39) Wang, T.; Chen, C.; Larcher, L. M.; Barrero, R. A.; Veedu, R. N. Three Decades of Nucleic Acid Aptamer Technologies: Lessons Learned, Progress and Opportunities on Aptamer Development. *Biotechnol. Adv.* **2019**, *37*, 28−50.
(40) Banerjee, J.; Nilsen-Hamilton, M. Aptamers: Multifunctional Molecules for Biomedical Research. *J. Mol. Med.* **2013**, *91*, 1333−1342.
(41) Youn, H.; Lee, K.; Her, J.; Jeon, J.; Mok, J.; So, J.; Shin, S.; Ban, C. Aptasensor for Multiplex Detection of Antibiotics Based on FRET Strategy Combined with Aptamer/Graphene Oxide Complex. *Sci. Rep.* **2019**, *9*, 7659.
(42) Yu, H.; Alkhamis, O.; Canoura, J.; Liu, Y.; Xiao, Y. Advances and Challenges in Small-Molecule DNA Aptamer Isolation, Characterization, and Sensor Development. *Angew. Chem., Int. Ed.* **2021**, *60*, 16800−16823.
(43) Radi, A.-E.; O'Sullivan, C. K. Aptamer Conformational Switch as Sensitive Electrochemical Biosensor for Potassium Ion Recognition. *Chem. Commun.* **2006**, 3432−3434.
(44) Chung, S.; Sicklick, J. K.; Ray, P.; Hall, D. A. Development of a Soluble KIT Electrochemical Aptasensor for Cancer Theranostics. *ACS Sens.* **2021**, *6*, 1971−1979.
(45) Idili, A.; Gerson, J.; Parolo, C.; Kippin, T.; Plaxco, K. W. An Electrochemical Aptamer-Based Sensor for the Rapid and Convenient Measurement of L-Tryptophan. *Anal. Bioanal. Chem.* **2019**, *411*, 4629−4635.
(46) Liu, J.; Cao, Z.; Lu, Y. Functional Nucleic Acid Sensors. *Chem. Rev.* **2009**, *109*, 1948−1998.
(47) Wang, C.; Li, Y.; Zhao, Q. A Signal-on Electrochemical Aptasensor for Rapid Detection of Aflatoxin B1 Based on Competition with Complementary DNA. *Biosens. Bioelectron.* **2019**, *144*, 111641.
(48) Yousefi, M.; Dehghani, S.; Nosrati, R.; Zare, H.; Evazalipour, M.; Mosafer, J.; Tehrani, B. S.; Pasdar, A.; Mokhtarzadeh, A.; Ramezani, M. Aptasensors as a New Sensing Technology Developed for the Detection of MUC1 Mucin: A Review. *Biosens. Bioelectron.* **2019**, *130*, 1−19.
(49) Schoukroun-Barnes, L. R.; Macazo, F. C.; Gutierrez, B.; Lottermoser, J.; Liu, J.; White, R. J. Reagentless, Structure-Switching, Electrochemical Aptamer-Based Sensors. *Annu. Rev. Anal. Chem.* **2016**, *9*, 163−181.
(50) Wang, J.; Gong, Q.; Maheshwari, N.; Eisenstein, M.; Arcila, M. L.; Kosik, K. S.; Soh, H. T. Particle Display: A Quantitative Screening Method for Generating High-Affinity Aptamers. *Angew. Chem., Int. Ed.* **2014**, *53*, 4796−4801.
(51) Schütze, T.; Wilhelm, B.; Greiner, N.; Braun, H.; Peter, F.; Mörl, M.; Erdmann, V. A.; Lehrach, H.; Konthur, Z.; Menger, M.; Arndt, P. F.; Glökler, J. Probing the SELEX Process with Next-Generation Sequencing. *PLoS One* **2011**, *6*, No. e29604.
(52) Kikin, O.; D'Antonio, L.; Bagga, P. S. QGRS Mapper: A Web-Based Server for Predicting G-Quadruplexes in Nucleotide Sequences. *Nucleic Acids Res.* **2006**, *34*, W676.
(53) Sefah, K.; Shangguan, D.; Xiong, X.; O'Donoghue, M. B.; Tan, W. Development of DNA Aptamers Using Cell-SELEX. *Nat. Protoc.* **2010**, *5*, 1169−1185.
(54) Wang, S.; Zhang, J.; Gharbi, O.; Vivier, V.; Gao, M.; Orazem, M. E. Electrochemical Impedance Spectroscopy. *Nat. Rev. Methods Primers* **2021**, *1*, 41.
(55) Jo, H.; Kim, S.-K.; Youn, H.; Lee, H.; Lee, K.; Jeong, J.; Mok, J.; Kim, S.-H.; Park, H.-S.; Ban, C. A Highly Sensitive and Selective Impedimetric Aptasensor for Interleukin-17 Receptor A. *Biosens. Bioelectron.* **2016**, *81*, 80−86.
(56) White, R. J.; Phares, N.; Lubin, A. A.; Xiao, Y.; Plaxco, K. W. Optimization of Electrochemical Aptamer-Based Sensors via Optimization of Probe Packing Density and Surface Chemistry. *Langmuir* **2008**, *24*, 10513−10518.
(57) Li, J. J.; Fang, X.; Tan, W. Molecular Aptamer Beacons for Real-Time Protein Recognition. *Biochem. Biophys. Res. Commun.* **2002**, *292*, 31−40.
(58) Lee, S.; Song, K.-M.; Jeon, W.; Jo, H.; Shim, Y.-B.; Ban, C. A Highly Sensitive Aptasensor towards Plasmodium Lactate Dehydrogenase for the Diagnosis of Malaria. *Biosens. Bioelectron.* **2012**, *35*, 291−296.
(59) Dauphin-Ducharme, P.; Plaxco, K. W. Maximizing the Signal Gain of Electrochemical-DNA Sensors. *Anal. Chem.* **2016**, *88*, 11654−11662.
(60) Mirceski, V.; Komorsky-Lovric, S.; Lovric, M. *Square-Wave Voltammetry: Theory and Application*; Springer Science & Business Media, 2007.
(61) Upan, J.; Youngvises, N.; Tuantranont, A.; Karuwan, C.; Banet, P.; Aubert, P.-H.; Jakmunee, J. A Simple Label-Free Electrochemical Sensor for Sensitive Detection of Alpha-Fetoprotein Based on Specific Aptamer Immobilized Platinum Nanoparticles/Carboxylated-Graphene Oxide. *Sci. Rep.* **2021**, *11*, 13969.
(62) Zamay, G. S.; Zamay, T. N.; Kolovskii, V. A.; Shabanov, A. V.; Glazyrin, Y. E.; Veprintsev, D. V.; Krat, A. V.; Zamay, S. S.; Kolovskaya, O. S.; Gargaun, A.; Sokolov, A. E.; Modestov, A. A.; Artyukhov, I. P.; Chesnokov, N. V.; Petrova, M. M.; Berezovski, M.

https://doi.org/10.1021/acsomega.2c04865
ACS Omega 2022, 7, 39097−39106

V.; Zamay, A. S. Electrochemical Aptasensor for Lung Cancer-Related Protein Detection in Crude Blood Plasma Samples. *Sci. Rep.* **2016**, *6*, 34350.
(63) Shaver, A.; Kundu, N.; Young, B. E.; Vieira, P. A.; Sczepanski, J. T.; Arroyo-Currás, N. Nuclease Hydrolysis Does Not Drive the Rapid Signaling Decay of DNA Aptamer-Based Electrochemical Sensors in Biological Fluids. *Langmuir* **2021**, *37*, 5213−5221.
(64) Leung, K. K.; Downs, A. M.; Ortega, G.; Kurnik, M.; Plaxco, K. W. Elucidating the Mechanisms Underlying the Signal Drift of Electrochemical Aptamer-Based Sensors in Whole Blood. *ACS Sens.* **2021**, *6*, 3340−3347.
(65) Ishikawa, R.; Yasuda, M.; Sasaki, S.; Ma, Y.; Nagasawa, K.; Tera, M. Stabilization of Telomeric G-Quadruplex by Ligand Binding Increases Susceptibility to S1 Nuclease. *Chem. Commun.* **2021**, *57*, 7236−7239.
(66) Stability and kinetics of G-quadruplex structures|Nucleic Acids Research; Oxford Academic. https://academic.oup.com/nar/article/36/17/5482/2410379 (accessed March 27, 2022).
(67) Kratschmer, C.; Levy, M. Effect of Chemical Modifications on Aptamer Stability in Serum. *Nucleic Acid Therapeut.* **2017**, *27*, 335−344.

https://doi.org/10.1021/acsomega.2c04865
ACS Omega 2022, 7, 39097−39106